Photoinduced structural changes in amorphous As_2S_3 as measured by differential anomalous x-ray scattering

Qing Ma, Weiqing Zhou, D. E. Sayers, and M. A. Paesler*
Department of Physics, Cox Hall, Box 8202, North Carolina State University, Raleigh, North Carolina 27695
(Received 10 March 1995)

Differential anomalous x-ray scattering measurements were made on a well-annealed and a photodarkened amorphous As_2S_3 film of 4 μm in thickness as well as on a well-annealed 30 μm sample, all of which were supported on Si (100) wafers. The thicker sample was used to evaluate the influence of x-ray scattering from the Si wafer. From the data measured, no structural change was found in the first coordination shell after light exposure. There is also no significant change in the region around 3.5 Å as far as the interatomic distances and coordination numbers are concerned, but a large increase in the disorder is seen, after illumination. The variation of the S apex angle for the As-S-As correlation is increased by about 2.4°. It is proposed that this is the fundamental cause for the reversible photodarkening observed in a-As_2S_3 films. The model developed based on these results explains many of the observations regarding the reversible photodarkening phenomenon, such as the dependence on light exposure, pressure, and the light intensity, and on the chalcogen concentration. It may also apply to other light-sensitive disordered materials. The present model establishes a clear relation between a local event, viz., the increased spread in the bond angle, and the matrix reorganization that affects a longer-range order, such as that responsible for the first sharp diffraction peak.

I. INTRODUCTION

It is well known that a redshift in the optical absorption gap upon photon illumination is observed over a limited range of composition for amorphous As_xS_{1-x} films. This so-called photodarkening may be irreversible or reversible depending on whether the film is well annealed or not before photon exposure. Studies[1–3] using x-ray absorption spectroscopy (XAS) have provided a detailed description of the local order and showed that amorphous and crystalline As_2S_3 have a similar local structure or short-range order (SRO). These studies also reported evidence of the existence of homopolar As-As bonds in a-As_2S_3 and their evolution upon illumination as well as a slight enlargement of the S apex bond angle.[1] Other studies, using x-ray scattering,[4–7] neutron scattering,[8] and Raman scattering,[9–11] as well as x-ray near absorption edge fine structure (XANES),[12] present evidence of intermediate-range order (IRO) in a-As_2S_3. The changes due to photosoaking observed in the first sharp diffraction peak[13] (FSDP) and in the small peak on the high-energy side of the white line in the XANES (Ref. 12) are considered to be evidence of the IRO. Based on the structural changes observed, microscopic mechanisms, such as bond breaking or switching, twisting of the bond angle, and modification of the IRO, have been suggested.

Despite a great number of studies of the atomic structure,[14,15] the microscopic mechanism responsible for the photoinduced structural changes is still not well understood, as pointed out by Tanaka[16] in a recent review paper. The model based on atomic bonding configuration change, first suggested by Street[17] and recently detailed by Fritzsche,[15] is quite commonly cited. This model and others will be reviewed in the discussion section of this paper.

The study carried out by Yang, Paesler, and Sayers[3] using the XAS technique showed that the second shell structure in the photodarkened film is more disordered than in the annealed film. This is a significant observation. However, the information contained in the extended x-ray absorption fine structure (EXAFS) signal in this region is rather weak due to the disorder in these amorphous materials. This limits the quantitative information which can be obtained about bond angles. Previous anomalous x-ray-scattering data[18] indicated significant changes in structure, which are related both to the SRO and IRO, when the different scattering patterns for the annealed and photodarkened samples were compared. In this paper, quantitative results are obtained through analysis of recently measured x-ray-scattering data in an attempt to achieve more structural information about the second nearest shell and bond angles. Differential anomalous x-ray-scattering (DAXS) measurements were performed at several x-ray wavelengths around the As K edge on a thermally annealed and a photodarkened a-As_2S_3 films. This effort represents a continuation of earlier work[18] to discuss the physical relationship between structural changes and the reversible photodarkening phenomenon.

The scattered intensity varies with energy E of the incident x-ray beam due to the energy dependence of the atomic scattering factor $f(q,E)=f_0(q)+f'(E)+if''(E)$, where $q=4\pi\sin\theta/\lambda$ is the scattering vector. When the x-ray energy is tuned near an absorption edge of one of the atomic species in a material, the variation may be significant. This can produce a substantial contrast among the scattering patterns recorded at different x-ray wavelengths. The contrast can be used to obtain a differential structure factor[19] (DSF) by taking the difference of two scattering patterns measured, typically,

at several electron volts and several hundred electron volts below the absorption edge. This difference eliminates information about other pair correlations except those involving the atomic species around whose absorption edge the measurement is made. For a binary alloy AB, the DSF will contain only the A-B and A-A correlations if the measurement is performed around the absorption edge of A, since the atomic scattering factor of B does not change significantly over the energy range used and thus the B-B contribution is eliminated in the difference. Like EXAFS, DAXS thus provides selective information about the structural environment around a specific atomic species. But, it is more sensitive to the IRO.

A description of the experiment is presented in Sec. II and the data analysis procedure will be described in Sec. III. Structural results are presented in Sec. IV. A model for reversible photodarkening based on the structural results reported in this paper is proposed in Sec. V. We conclude in Sec. VI.

II. EXPERIMENTAL

The experimental details have been presented elsewhere.[18] Only a brief description about sample preparation and data collection will be presented here.

A. Sample preparation

The as-deposited a-As_2S_3 films were prepared by evaporating bulk glass As_2S_3 (of purity 99.99% manufactured by CERAC) in a diffusion-pumped and cold-trapped system. The deposition rates for the samples used in this study were about 20 Å per second. The vacuum pressure during evaporation was less than 10^{-6} torr. The substrate temperature was room temperature. A c-Si (100) wafer was used as the substrate material. After deposition, the thin films were moved into a separate annealing chamber. Annealing was done with the sample in the dark at 445 K for 1 h in a flow of high-purity argon gas. Then, through a slow cooling cycle, the temperature of the samples was brought back to room temperature. To study the photoinduced structural change, one annealed sample was then photodarkened by an exposure to an Ar laser beam (488 nm and 100 mW) for more than 20 min at 77 K. Two 4 μm samples were prepared, one of which was well annealed and the other photodarkened after annealing. One 30 μm sample which was well annealed was used to evaluate the substrate effect on the scattering patterns of the thinner samples. After photosoaking, the samples show changes in their Raman spectra, optical absorption edge, and thicknesses which are in good agreement with previously reported results.

B. Data collection

The DAXS experiments were carried out in the vicinity of the As K edge (11 867 eV) using the x-ray beam from the superconducting wiggler at DCI in LURE. A double-crystal [Si(220)] monochromator was employed to select the beam energy. The temperature of the first crystal was controlled at about 12 °C. The sample was mounted on a two-circle vertical diffractometer and fixed at a small angle of 1.5°, which is the angle between the surface of the sample and the incident beam. The vertical and horizontal sizes of the incident beam are defined by a slit of 0.8×10 mm before the sample and the incident x-ray intensity I_0 was monitored by scattering a small amount of beam using a plastic film into a NaI scintillation detector. I_0 was used to eliminate the time-dependent variation of intensity of the synchrotron radiation beam. The scattering in the vertical plane was collected by a multielement solid-state detector which consists of 12 parallel Si:Li plates, each one acting as an independent detector. A radial slit system, which was specifically designed for this detector, was put just in front of the detector to reduce spurious scattering signals. When the x-ray photon energy is tuned in the vicinity of an absorption edge, the use of such an energy-sensitive detector allows simultaneous measurement of the scattered intensity I_s (including the elastic and Compton scattering as well as the K_β fluorescence contribution), and the K_α fluorescence intensity I_α. This allows the contribution of the K_α fluorescence to be separated out experimentally. The K_β fluorescence intensity is then subtracted from the scattered intensity using the ratio value I_β/I_α determined from a measurement at an x-ray photon energy of 26 800 eV, which is far above the absorption edge so that the K_β component can be resolved from the elastically scattered radiation. The scattering pattern was recorded using a step size of 0.05 Å^{-1} in q and a time interval of 15 sec per point. Each element of the detector was running within its linear range since the counting rate was typically lower than 3000 counts per second for each channel.

The energies and corresponding values of the energy-dependence terms $f'(E)$ and $f''(E)$ of the atomic scattering factors used for our measurements are given in Table I. $f''(E)$ values near the edge determined from EXAFS measurements which were performed on the same samples. $f'(E)$ values around the edge were calculated from $f''(E)$ using the Kramers-Kronig relationship. In this calculation, the $f''(E)$ values determined from the absorption experimental data were matched to values calculated by Sasaki[20] for free atoms over an energy range from ~4 to ~120 keV to meet the requirement of a large integration range.[21] $f'(E)$ and $f''(E)$ values far from the edge were taken directly from Sasaki's data. The DSF's for the As_2S_3 samples were obtained by taking the differences of intensities measured at energies of 11 650 and 11 860 eV.

TABLE I. f' and f'' values (electron units) of As, S, and Si atoms at energies used.

Energy (eV)	f'_{As}	f''_{As}	f'_{S}	f''_{S}	f'_{Si}	f''_{Si}
11 650	−4.00	0.50	−0.23	0.33	0.16	0.19
11 860	−9.20	0.50	−0.23	0.33	0.17	0.19
26 800	0.01	1.91	0.09	0.12		0.07

III. DATA ANALYSIS

The atomic radial distribution function (RDF) about an average atom,

$$4\pi r^2\rho(r)=4\pi r^2\rho_0+r\int q[S(q)-1]\sin(qr)dq \ . \quad (1)$$

where $\rho(r)$ and ρ_0 are the radial and average densities in atoms/Å^3, respectively, and $S(q)$ is the structure factor, which is related to the elastically scattered intensity by

$$I_s(q,E)=\langle f(q,E)^2\rangle-\langle f(q,E)\rangle^2+\langle f(q,E)\rangle^2 S(q) \ , \quad (2)$$

in which $\langle\ \rangle$ represents the chemical average of the atomic scattering factors. In a binary system $S(q)$, in turn, can be written as a linear combination of three partial structure factors $S_{ij}(q)$ weighted by factors $W_{ij}(q,E)$, viz.,

$$W_{ij}(q,E)=c_i c_j\frac{f_i(q,E)f_j(q,E)}{\langle f(q,E)\rangle^2} \ , \quad (3)$$

in which c_i is the atomic fraction of the atomic species i. W_{ij} is called the weighting factor. It is a measure of the contribution of each of the atomic correlations to the scattered intensity and varies with energy. Analogously, the differential structure factor $\Delta S(q)$ is related to the difference of the intensities measured at two energies by the relationship

$$\begin{aligned}\Delta I&=I(q,E_1)-I(q,E_2)\\&=\Delta_A[\langle f^2\rangle-\langle f\rangle^2]+\Delta_A[\langle f\rangle^2]\Delta S(q) \ , \end{aligned}\quad (4)$$

where A specifies the atomic species around whose absorption edge $I(q,E_1)$ and $I(q,E_2)$ were measured and Δ represents the difference. $\Delta S(q)$ is thus a linear combination of the two atom A related partial structure factors, i.e., S_{AA} and S_{AB}, weighted by

$$W_{ij}(q,E)=c_i c_j\frac{\Delta_A(f_1(q,E)f_j(q,E))}{\Delta_A\langle f(q,E)\rangle^2} \ . \quad (5)$$

The Fourier transform of ΔS yields the differential radial distribution function about atom A. For a multicomponent sample, this function is a convolution of the real distribution functions $D_{ij}(r)$ with their weighting factors ω_{ij}, viz.,

$$4\pi r^2\rho(r)=\sum_{j,i=1,i\le j}^{2}\omega_{ij}(r)^*D_{ij}(r) \ , \quad (6)$$

in which ω_{ij} is the Fourier transform of the weighting factors W_{ij}. To first order, $\omega_{ij}=W_{ij}/c_i$. Using this approximation, the integral of a peak in the radial distribution function can be written as

$$\int_{r_1}^{r_2}4\pi r^2\rho(r)dr\sim\sum_{j,i=1,i\le j}^{2}\frac{W_{ij}}{c_i}N_{ij} \ , \quad (7)$$

where N_{ij} is the coordination number of j about i. In practice, the structural parameters are determined by an iterative analysis procedure, for which the peak of the radial distribution function is assumed to have the form of a pseudo-Gaussian distribution function, viz.:

$$P_{ij}(r)=\frac{1}{r_0\sigma\sqrt{2\pi}}N_{ij}(e^{-(r-r_0)^2/2\sigma^2}-e^{-(r+r_0)^2/2\sigma^2}) \ , \quad (8)$$

Given the average interatomic distance r_0, the coordination number N_{ij}, and the Gaussian width σ, $P_{ij}(r)$ is Fourier transformed into q space, and the result is multiplied by the corresponding $W_{ij}(q)$ factor. This gives the contribution of one kind of correlation to $\Delta S(q)$. This result is then Fourier transformed back to r space, yielding one partial distribution function. In this operation, the same q ranges were used in the Fourier transform as for the experimental data so that truncation effects should be similar. This function can be compared to the experimentally obtained distribution function. The parameters which yield the best comparison to the measured data are used to interpret the structure. All of the structural parameters presented here were obtained in such a way.

Obviously, the truncation effect resulted in termination errors since the Fourier transforms were performed in a limited q range. In order to deal with such errors, a convergence factor $\exp(-\alpha^2q^2)$ ($\alpha^2=0.005$) was added to the interference function, which could rather effectively reduce the contribution of the high-q values and, thus, the termination errors.[22] The experimental raw data were measured up to 10 Å^{-1}. However, the ending part did not present a node and the last node in the interference functions was located at 8.2 Å^{-1}. The termination at the node resulted in much less errors than at 10 Å^{-1}, as checked. Thus, to be consistent, the Fourier transforms are performed for all data over the same q range, namely, from 0.3 to ~8.2 Å^{-1}.

To obtain the elastically scattered intensity, the raw data have been treated using the following procedures: (1) the experimental scattering intensity is normalized relative to the incident beam intensity in order to remove any time dependence of the incident beam; (2) a geometrical absorption correction and an interactive volume correction is applied; (3) a polarization correction is made; (4) scattering from the silicon substrate is subtracted; (5) the K_β fluorescence is subtracted as described above (Sec. II B); (6) the inelastically scattered intensity is subtracted using theoretical values;[23] and finally, (7) the experimental data are normalized to a per electron scale.

IV. RESULTS

Figures 1 and 2 show the q dependence of weighting factors W_{ij} for the total structure factor (TSF) and the differential structure factor (DSF), respectively. A remarkable feature for the As_2S_3 alloy is that there is a dramatic change of the weighting factor for As-As correlations when passing between the TSF and the DSF of the As K edge, while the weighting factor for As-S correlations is only slightly changed. The weighting of the As-As correlations roughly doubles. These large differences between the TSF and DSF help to reliably determine the structure.

The TSF's obtained at energies of 11 650 eV (full line) and 11 860 eV (dotted line) for the annealed and photodarkened samples are shown in Figs. 3 and 4. A rather

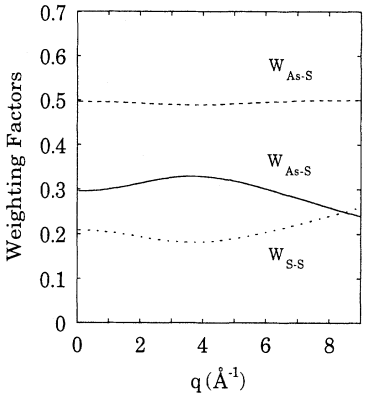

FIG. 1. Weighting factors of three atomic pairs in As_2S_3 vs q ($Å^{-1}$) in the TSF measured at an energy of 11 650 eV.

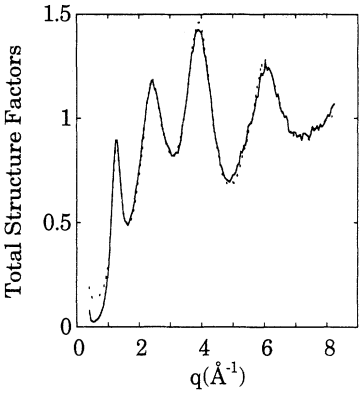

FIG. 4. TSF vs q ($Å^{-1}$) for the photodarkened sample, measured at energies of 11 650 eV (full line) and at 11 860 eV (dotted line).

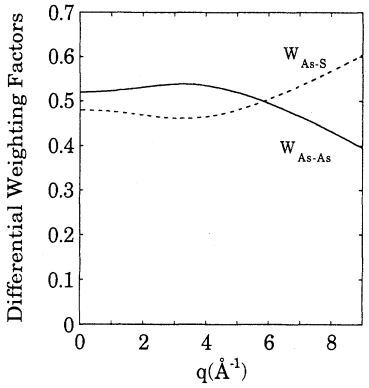

FIG. 2. Differential weighting factors vs q ($Å^{-1}$) for As-As and As-S atomic pairs. Weighting of As-As correlations is significantly increased relative to that in the TSF.

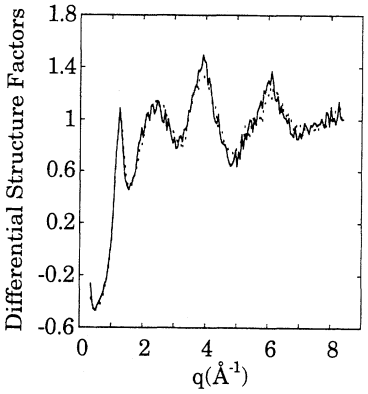

FIG. 5. DSF vs q ($Å^{-1}$) for the annealed (full line) and photodarkened (dotted line) samples.

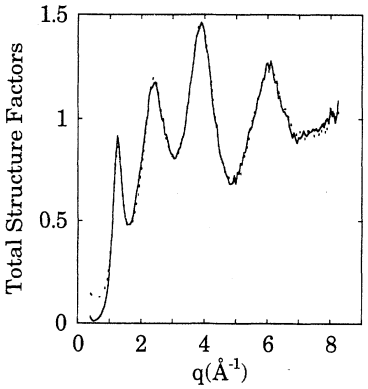

FIG. 3. TSF vs q ($Å^{-1}$) for the annealed thin sample, measured at 11 650 eV (full line) and at 11 860 eV (dotted line).

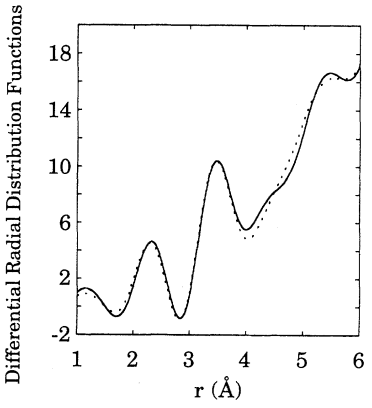

FIG. 6. DDF vs r (Å) for the thick (dotted line) and thin (full line) annealed samples.

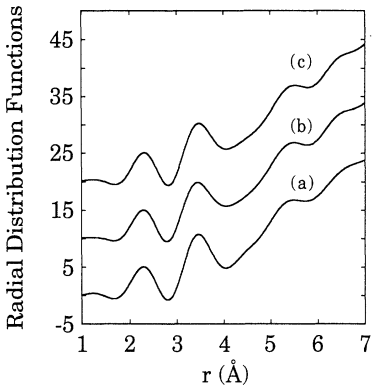

FIG. 7. RDF vs r (Å) for (a) 30 μm annealed sample, (b) 4 μm annealed sample, and (c) 4 μm photodarkened sample.

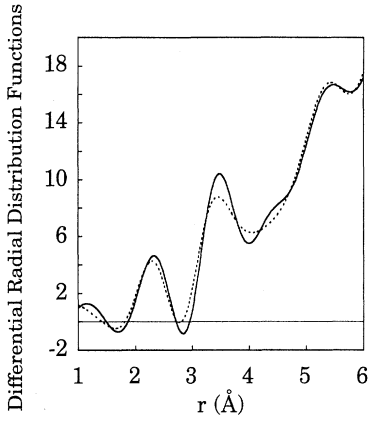

FIG. 8. DDF vs r (Å) for the annealed (full line) and photodarkened (dotted line) samples.

intense FSDF appears in the low-q range for both samples. It seems to be dominated by As-related correlations as was extensively discussed in Ref. 18. Figure 5 shows the DSF's obtained from the TSF's shown in Figs. 3 and 4. Because the DSF's are difference scattering patterns, the noise level is significantly enhanced. The high-frequency noise may cause a slight distortion in the high-r part of the radial distribution function. In order to check the influence of the substrate, we compare the differential distribution functions (DDF) for the annealed thick (full line) and thin (dotted line) samples in Fig. 6. They are very similar. This demonstrates that the DDF's for the thin samples are not strongly affected by scattering from the substrate.

A. First shell structure

Figure 7 shows the RDF's for the annealed thick (a), thin (b), and photosoaked (c) samples. Assuming that only As-S correlations contribute to the first peaks of the RDF's, coordination numbers, interatomic distances, and disorder parameters were obtained through the iterative procedure for the first shells, which are given in Table II. These results are in good agreement with those previously obtained by EXAFS, within ± 0.1 atom for the coordination number and ± 0.01 Å for the interatomic distance.[23] Figure 8 shows the DDF's for the annealed (a) and photosoaked (b) samples. The first peaks of the DDF's can be well fitted by using roughly the same parameters as obtained for the RDF's. The results are also presented in Table II. The precision is lower due to the poorer signal to noise ratio. A slight reduction is found for the coordination number for all the samples. This is likely to be due to systematic errors. However, there might be a slight reduction in magnitude of the first peak of the photosoaked sample relative to the annealed sample, as was shown in previous EXAFS results.[3]

There is no evidence for the possible existence of homopolar As-As bonds. Bearing in mind that the bond lengths for S-S, As-S, and As-As are substantially different, there is no peak position shift of the first shell observed when the RDF and DDF of either photosoaked or annealed sample are compared, although the weighting of As-As pairs increases by $\sim 50\%$ (See Fig. 1) for the DDF and although S-S pairs do not exist in the DDF. This strongly implies that the first shell consists primarily of As-S bonds. In a previous study of the bulk amorphous As_2Te_3, the existence of homopolar bonds is clearly demonstrated by the peak position shift.[24] The EXAFS studies of the well-annealed As_2S_3 film also find no As-As bonds in the structure.[23] EXAFS is sensitive to this since the phase shifts for As-As and As-S pairs are substantially different. Thus it is concluded that the three samples have an identical first shell and that no structural change in this shell induced by light exposure is detectable, at least by DAXS.

B. Second shell structures

As stated, the DDF's for the thick and thin annealed samples are almost identical. However, the DDF of the photosoaked sample has a noticeable change in the second shell in comparison with the DDF's of the annealed sample (See Fig. 8). The magnitude of the second shell peak is significantly reduced after light exposure. Indeed, the damping of oscillations in the DSF can also

TABLE II. Structural parameters for the first shell determined from the RDF's and DDF's.

Sample	$N\pm0.1$	$r\pm0.01$ (Å)	$\sigma\pm0.01$ (Å)	$N\pm0.2$	$r\pm0.02$ (Å)	$\sigma\pm0.01$ (Å)
		RDF's			DDF's	
30 μm	2.9	2.27	0.14	2.8	2.26	0.15
a-4 μm	2.9	2.27	0.14	2.8	2.28	0.16
p-4 μm	2.9	2.27	0.13	2.7	2.27	0.16

be seen (see Fig. 5). The immediate conclusion is that photosoaking of a well-annealed sample induces disorder in the second shell. This is in agreement with the observation made by EXAFS.[3] It is noticed that the second peaks in the RDF's for three samples are rather identical in their shape and that the second peaks in the DDF's for the annealed samples have almost the same shape as the corresponding RDF's, but this is not the case for the photodarkened sample. Since the weighting factor for As-As pairs from the TSF to the DSF is significantly increased and since for As-S pairs, it remains almost unchanged, it is therefore expected that the change in the peak shape is related predominantely to As-As correlations for which there is a larger disorder. In the crystalline As_2S_3 orpiment structure, the second shell distance for As-As pairs is larger by ~ 0.2 Å than for As-S pairs.[25] It is also likely that in a-As_2S_3, the average length of As-As correlations is larger than that of As-S correlations so that the shape of the second peak of the photosoaked sample can be well understood.

The EXAFS studies found three As-As pairs in the second shell, while As-S correlations were not observed.[3] For the DAXS data, we assumed three As-As pairs to fit the second shell of the DDF for the thick annealed sample. However, they filled only half of the area. This suggests that the DAXS data contains a substantial contribution from As-S correlations. Thus, As-S pairs were added until the whole area was fit. The result shows three As-S pairs contributing. The structural parameters found for this sample can be applied to the thin annealed sample with a slight variation, as shown in Table III. Figure 9(a) shows the fit of the DDF for the thin sample. The third peak is constructed only to approximate the effect of higher shells, but no parameters are deduced for it.

We then reconstructed the second shell peak of the photosoaked sample using similar distances and coordination numbers to those used for the annealed samples. Figure 9(b) shows the fitting quality of the first two shells of the DDF of this sample. The structural parameters obtained are also presented in Table III. It can be seen that larger disorder parameters were used. To account for the slight shift of the second peak position to lower distances, the σ value for As-As correlations was found to be slightly larger than the σ for As-S correlations.

As stated above, the contrast between the TSF and DSF can be used to distinguish structural information. Using the results determined from the DDF's, the RDF for each sample can be analyzed. In this analysis, the structural parameters for As-As and As-S pairs were kept at similar values to those from the DDF's. Assuming only As-As and As-S pairs in the second shell is not

TABLE III. Structural parameters for the secnod shell in the DDF's.

Sample	$N\pm0.2$		$r\pm0.02$ (Å)		$\sigma\pm0.01$(Å)	
	As-S	As-As	As-S	As-As	As-S	As-As
30 μm	3.1	3.0	3.40	3.53	0.22	0.22
a-4μm	3.0	3.0	3.40	3.53	0.22	0.22
p-4μm	3.2	3.2	3.37	3.53	0.28	0.30

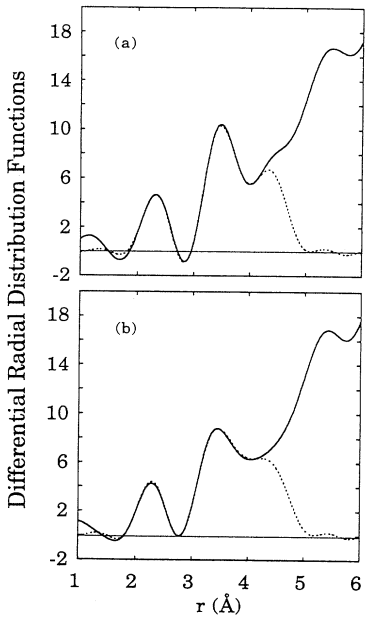

FIG. 9. Reconstructions (dotted line) of the first two shells for (a) the annealed sample and (b) the photodarkened sample.

sufficient to fit the whole peak area in the RDF as shown, for example, in Fig. 10. This implies that the second shell contains S-S correlations as well. Thus, six S-S pairs were added to account for the difference. The results are shown in Table IV. The S-S pairs in the second shell appear to be unchanged from the annealed to the photosoaked sample, indicating that the disordering, observed for the latter, is due dominantly to As-related correlations and, thus, a disorder of the S apex bond angles. For the annealed samples, it appears that the σ values have to be slightly increased to get a better correspondence with the data.

Error bars for coordination numbers, Gaussian widths, and interatomic distances obtained above are estimated by comparing structural parameters determined from the RDF's and DDF's. For the distances, it is found to be within ±0.02 Å, for the coordination number within

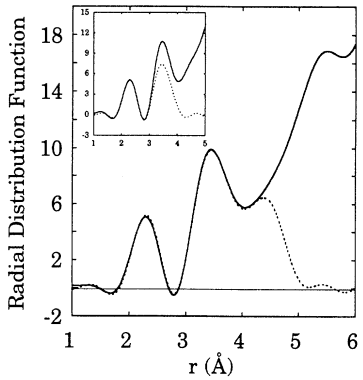

FIG. 10. Reconstructions (dotted line) of the first two shells of the RDF; inset is reconstruction with only the As-As and As-S pairs involved.

TABLE IV. Structural parameters for the second shell in the RDF's.

Sample	$N\pm0.2$			$r\pm0.02$(Å)			$\sigma\pm0.01$(Å)		
	As-S	S-S	As-As	As-S	S-S	As-As	As-S	S-S	As-As
30 μm	3.1	6.1	3.1	3.40	3.47	3.55	0.24	0.24	0.24
a-4 μm	3.1	6.0	3.1	3.41	3.47	3.55	0.24	0.24	0.25
p-4 μm	3.2	6.1	3.2	3.39	3.46	3.55	0.28	0.24	0.30

±0.2 atoms, and for the Gaussian width within ±0.01 Å. Errors caused by other sources, such as the possible inaccurate estimation of the sample density, are well within the given error bars.

From the first and second shells the bond angles θ_{AsSAs} or θ_{SAsS} were calculated using 2.27 Å for the first shell, 3.46 Å for the S-S pair, and 3.54 Å for the As-As pair. We find $\theta_{AsSAs}=102.5°$ and $\theta_{SAsS}=99.5°$. The latter is 99° in the crystalline structure, θ_{AsSAs} is slightly larger than that observed by EXAFS.[3] However, what is significant, we believe, is the relative change upon light exposure. Assuming that the thermal effect on the disorder is the same for both samples, the difference observed in σ is thus due only to a static change in disorder, which can be calculated by

$$\Delta\sigma=\frac{\sigma_p^2-\sigma_a^2}{\sigma_p+\sigma_a}\ , \tag{9}$$

where σ_p is for the photodarkened sample and σ_a for the annealed sample. Since σ_p is equal to 0.24, if an average of the results determined from the DDF and RDF is taken, and σ_a to 0.30, the difference $\Delta\sigma$ is equal to 0.06 Å. This value indicates an increased spread of about 2.4° in the S apex bond angle θ_{AsSaS} after light exposure.

Information regarding the structure beyond the second shell can be obtained by extracting the partial structure factors, which requires data with a better signal to noise ratio than reported here. The results presented above are significant as far as the relative change between the structures of the photodarkened and annealed samples is concerned.

V. DISCUSSION

From the DAXS data, detailed information about the SRO in a well-annealed and a photosoaked As_2S_3 film was obtained. The SRO in these samples is chemically ordered and is rather similar to the structure of the crystalline As_2S_3. No structural change after light exposure in the first shell is detected, and thus it is concluded that the first shell remains identical in both samples. The As-related correlations in the second shell show a strong disordering after light exposure, but no significant change either in distance or in coordination number. The increased disorder observed for As-S correlations is believed to be associated with the disordering of As-As correlations and thus the S apex bond angle. It is proposed that the reversible photoinduced structural change is related to changes in the S apex bond angle, upon photosoaking or annealing, and that the redshift in the optical absorption edge and other properties, therefore, is also due to this structural change.

A. The model based on the valence alternation D^+D^- pairs

Mott and Stoneham[26] pointed out that the exciton generated by photon absorption can exist either in a state without the matrix distortion or in a state where a strong distortion occurs and the exciton is self trapped. Based on this, Street[17] and several other authors[15] proposed a model to explain the reversible photoinduced structural change occurring in chalcogenide glasses. The lone pair p electrons of the chalcogen are localized in the band tail of the valence band and are easily excited, usually by light exposure using a photon energy close to the band gap (E_g). According to Street, the exciton thus generated can be either self trapped in a localized state, which has higher energy than the ground state, or can recombine back to the ground state. He argued that the energy level of the trap should be considerably lower in comparison with that of the exciton so that the energy barrier from the exciton level to the trap is small. The filled trapped state is the cause of the redshift. Its higher energy is due to the strengthening of the localized state by the creation of a kind of defect in the atomic bonding configuration, such as the so-called valence alternation pairs described by Kastner, Adler, and Fritzsche.[27] This has been widely accepted as a possible mechanism for photodarkening. The basic assumptions for this are that the atomic bonding configuration can be altered due to illumination, resulting in, locally, an overcoordinated center with a positive charge (D^+) and an undercoordinated center with a negative charge (D^-), simultaneously, and that the energy of the resulting D^+,D^- pair is higher by a small amount (a fraction of E_g) than the ground state. Thermal annealing will relax the light-induced defect and excite the trapped exciton back to the ground state, resulting in bleaching.

A typical example used to support this model is selenium (Se), which has a chain structure with an interchain distance of about 3.5 Å. In this case, a D^+,D^- pair is formed by a threefold-coordinated Se atom and a singly coordinated Se atom. Kastner extended this to the system involving a pnictide atom (As) and a chalcogen atom by arguing that the s-like lone pair electrons on the pnictide atom can play a similar role as the lone pair in Se. Fritzsche[15] extended this model to explain how the relaxation of the exciton depends on experimental parameters, such as the exposure temperature, pressure, and the light intensity.

Our results do not support this D^+,D^- photodarken-

ing. The densities necessary to result in photodarkening are well beyond our detection limit. According to Ref. 17, the density of defects in chalcogenides is estimated to be 10^{17} to 10^{18} cm^{-3}. Such a density of 10^{-7} to 10^{-6} $Å^{-3}$ corresponds to one defect in a volume of 10^7 or 10^6 $Å^3$. For the As_2S_3 thin-film density of 3.89×10^{-2} atom/$Å^3$ (3.18 g/cm^3) and a partial S density of 2.33×10^{-2} atom/$Å^3$, the corresponding defect concentration is less than 0.01%. This value is not only well beyond the detection limit, it is also a number suspiciously small to be expected to lead a matrix-related band-gap effect such as photodarkening. There are other recent structural results which also challenge the D^+,D^- model. We discuss these in the following pages. Based on the structural results reported in this paper, we propose a model to explain the photodarkening and phenomena associated with it.

B. A proposed model based on the new structural results

In light of the principles of creation of the exciton and of its recombination processes suggested by Mott and Stoneham,[26] we propose that the increased disorder of the S apex bond angle after light exposure occurs by the following mechanism:

(a) As is known, the band of the lone pair electrons sits just on the top of the valence band, being a localized state. The light excites the lone pair electrons and excitons are created, thus changing the electrical screening locally around the chalcogen atom.

(b) The atomic arrangement responds to this through fluctuations of the bond angle, most likely the one on the chalcogen atom which is in the immediate vicinity of the absorption event.

(c) The disorder of the bond angle in turn strengthens the localized state by enhancing its energy a small amount (a fraction of E_g).

(d) Finally, the exciton recombines back to the energy-enhanced localized state if the disorder is stably established, or recombines back to the ground state (the undisturbed localized state) if the disorder is not stably established, and relaxes completely. In either case, the electron-phonon coupling assists the process.[17] Which rate is larger depends on the stability of the created disorder.

The present model can explain the observed reversible photoinduced phenomenon as does the D^+,D^- model. Similar to the explanation given by Fritzsche[15] using the D^+,D^- model, the present model also predicts that under illumination the light-saturated state is in dynamic equilibrium. The light-saturated state is reached once the increased disordered state is established. When light exposure is performed at temperatures higher than that used in the usual photodarkening procedure, a partial annealing occurs, under illumination as well as at elevated temperature, that causes the thermal relaxation of the light-induced bond angle disorder, and results in a partial bleaching.[28] In another words, heating destabilizes the light-induced bond angle disorder and reduces the probability for excitons to recombine back to the energy-enhanced localized state. This results in a smaller redshift for light exposure at elevated temperature. This is also the mechanism for bleaching when the annealing procedure is applied.

As pointed out by Fritzsche,[15] reversible photodarkening is usually accompanied by a reversible increase in volume. He suggested that this is related to the increased repulsive interaction in the more disordered state between the filled lone pair orbitals. As observed by Tanaka,[29] increasing the external pressure can produce the redshift as well, with a decrease in volume. He argued that pressure also increases the lone pair interaction. The D^+,D^- model is unable to deal with this pressure-induced redshift.[15] Here we try to understand the pressure dependence in the context of the bond angle disorder. What are the consequences of the increased pressure with respect to the atomic arrangement of the structure? In the case of As_2S_3, a shortening of distances between the layers is expected since they interact via the weak van der Waals forces. Second, bond angle changes are likely to occur. It is harder, though not impossible, to postulate creation of the D^+,D^- pair under increased pressure, which compresses the structure as a whole, unlike light exposure for which electron excitation depends on a specific electronic structure. It is believed that the lone pair interaction is enhanced by disordering of the bond angle due to external pressure, but the sequence is different from that for light exposure. It is proposed that: (a) with increasing pressure, the bond angle changes; (b) outer electrons respond to the new potential by, most likely, increasing their energy, which is one way to transfer the energy due to the compression force, resulting in the redshift in the band gap; and (c) if the matrix distortion does not exceed the elastic regime, the redshift is reversible. Thus, either for light exposure or increased pressure, the enhancement of lone pair interaction seems to be the underlying cause of the redshift.[15,29]

This mechanism, plus that for light exposure, fits well to the light-induced redshift under pressure as demonstrated by Pfeiffer and Paesler[30] for As_2S_3. Pfeiffer and Paesler observed a sharp increase of the redshift in the low-pressure regime (1–5 kbar) and then a rapid decrease of it with pressure that approached zero at 60 kbar. In the particular case of As_2S_3, the presence of external pressure creates the bond angle disorder as well as helps to stabilize the light-induced bond angle disorder, and thus, the probability for excitons to recombine back to the energy-enhanced localized state is increased. This results in an increased amount of the redshift with pressure in the low-pressure region. With an increase of pressure, the further disordering of bond angles becomes hard and the response events of the bond angle disorder to electron excitation by light become few under higher pressure. Thus, the higher-energy state of the localized states is hard to stabilize or be populated. This results in the rapid decrease in the amount of the redshift with pressure.

Next, the chalcogen element dependence of the photodarkening phenomenon is examined in order to see if the D^+,D^- model applies. The observation of a threefold-coordinated tellurium (Te) site in liquid Te[31,32] was considered experimental evidence that supports the valence alternation mechanism.[27] However, a study by Mellene,

Bellissent, and Flank[33] using neutron scattering showed that the mean coordination number is about 2.5 in liquid Te, indicating that half of the Te is threefold coordinated and that the other half is twofold coordinated. Singly coordinated Te sites thus must be very few, if any. The study of bulk As_xTe_{1-x} amorphous samples by Ma, Raoux, and Benazeth using EXAFS and DAXS found a mean coordination number around Te of ~ 2.4 starting out at the As_2Te_3 composition, indicating, also, that the majority of Te is either twofold or threefold coordinated. These results imply that creation of a threefold-coordinated site does not necessarily yield a singly coordinated site and that a mean coordination number of ~ 2.4 around Te leaves little probability for existence of such a site. We expect an intermediate situation for the As_2Se_3 alloy, but a structural study addressing this question has not yet been done. Due to the existence of a large amount of threefold Te sites, the matrix should be more connected, rendering it difficult to deform, and the probability of recombination of excitons into the energy-enhanced localized states is smaller. This explains why the magnitude of the reversible photodarkening is smallest for Te containing glasses and largest for S containing glasses.[34] Another example is As_4S_4, for which no redshift is observed. This is because of the highly connected structure of the As_4S_4 molecular cage.

The disordering of the S apex bond angle implies a local motion of the As atoms. The decrease in intensity of the FSDP, which is believed to be associated with the structure beyond the SRO,[36] after light exposure[35,29,18] is likely related to this motion. A large amount of x-ray-scattering data shows the existence of the FSDP in many amorphous materials including As or Ge chalcogenides. The study of the intensity variation of a given FSDP with x-ray photon energy demonstrated that it is cation-atom (e.g., As or Ge) related.[37,23,18] It is speculated here that the disordering of the S apex bond angle distorts the matrix, resulting in a decrease in intensity of the FSDP. The matrix organization in turn determines, in part, the degree of the bond angle disorder, the energy level of the localized state, and thus, the magnitude of the photodarkening. This is the reason that the FSDP is also correlated with the photodarkening phenomenon.[15] Changes in the S bond angle induced by illumination might at first glance appear to be too small to result in the observed darkening. A simple calculation suggests, however, that the relative change in volume ($\Delta V/V = 6\times 10^{-3}$)[14] concomitant with photodarkening must involve an opening of the structure, and furthermore that such a volume change would occur if the S bond angle were to change by as little as 2°. Such a change is not unreasonable given the increased disorder reported here.

Finally, the question as to why the photodarkening does not occur in the crystalline state is addressed. Like other models proposed previously,[38–40] the present model has a common feature. They all are only possible in an amorphous state, whose structure is strained in the long range, but is relatively flexible in the short range. The basic molecular units are oriented differently in the structure with respect to the strain vector, resulting in an isotropic characteristic on the macroscopic scale. The differences from one location to another allow a slight structural change, such as a change of bond angle, to occur. In the crystalline structure, the units are well ordered. Any local event that violates the basic arrangement, which is not strong enough to destroy the lattice, will be "suppressed." The type of disordering reported in this paper will not occur. Thus, no photodarkening phenomenon is observed in crystalline chalcogenide materials.

VI. CONCLUSIONS

A comparative structural study of a well-annealed and a photosoaked As_2S_3 thin film, both supported on *c*-Si(100) wafers, using the differential anomalous x-ray scattering technique, has been reported here. A detailed description of the short-range order and of the bond angles in the structure has been obtained. No evidence for any change in the first shell structure was observed after photosoaking. There were also no changes either in distances or coordination numbers of the second shell. However, a strong disordering of the As-related correlations, due to illumination, in the second shell was observed. The disordering of the S apex bond angle is increased by about 2.4°. These structural results, together with recent ones on other chalcogenide amorphous materials such as As_2Te_3 (Ref. 24) and liquid Te,[33] do not support changes in the atomic bonding configuration and thus the existence of valence alternation D^+, D^- pairs. Following the principle previously suggested by Mott and Stoneham,[26] a model is proposed to explain the reversible photodarkening phenomenon observed in the *a*-As_2S_3 thin film and chalcogenide containing amorphous materials.

Instead of an atomic bonding configuration change, the change of the S apex bond angle after light exposure or annealing accounts for the reversible photodarkening including its various experimental conditions and chalcogen element dependences. The present model is more general than previously proposed models.[38–40] Moreover, this model has established a clear relation between the bonding disorder, which is a local event, and the matrix organization that involves a longer-range order that is responsible for the FSDP.

ACKNOWLEDGMENTS

We would like to thank Dr. Brigitte Bouchet-Fabre at LURE for her assistance with the DAXS experiment. Thanks also go to Dr. Denis Raoux for allocating to us the beam time. Dr. Gerd Pfeiffer has carefully read the manuscript and his comments on it are greatly appreciated. This work was supported, in part, by the Mobil Research and Development Corporation.

*Author to whom correspondence should be addressed.
[1]C. Y. Yang, M. A. Paesler, and D. E. Sayers, Phys. Rev. B **36**, 9160 (1987).
[2]C. Y. Yang, M. A. Paesler, and D. E. Sayers, Phys. Rev. B **36**, 8122 (1987).
[3]C. Y. Yang, M. A. Paesler, and D. E. Sayers, Phys. Rev. B **39**, 10 342 (1989).
[4]A. J. Leadbetter and A. J. Apling, J. Non-Cryst. Solids **15**, 250 (1974).
[5]L. E. Busse, Phys. Rev. B **29**, 3639 (1984).
[6]K. Tanaka, J. Non-Cryst. Solids **119**, 254 (1990).
[7]M. F. Daniel, A. J. Leadbetter, A. C. Wright, and R. N. Sinclair, J. Non-Cryst. Solids **32**, 271 (1979).
[8]S. R. Elliott, T. Rayment, and S. Cummings, J. Phys. (Paris) (Colloq.) **43**, C9-35 (1982).
[9]H. Kawamura, F. Fukumasu, and Y. Hamada, Solid State Commun. **43**, 229 (1982).
[10]V. K. Malinovisky and A. P. Sokolov, Solid State Commun. **57**, 757 (1986).
[11]T. Arai, H. Kataura, H. Yasuoka, and S. Onari, J. Non-Cryst. Solids **77&78**, 1149 (1985).
[12]D. E. Sayers, C. Y. Yang, and M. A. Paesler, in *Disordered Semiconductors,* edited by M. A. Kastner, G. A. Thomas, and S. R. Ovshinsky (Plenum, New York, 1987), p. 173.
[13]Ke Tanaka, Appl. Phys. Lett. **26**, 243 (1975).
[14]G. Pfeiffer, M. A. Paesler, and S. C. Agarwal, J. Non-Cryst. Solids **130**, 111 (1991).
[15]H. Fritzsche, Philos. Mag. B **68**, 561 (1993).
[16]Ke Tanaka, Rev. Solid State Sci. **59&60**, 641 (1990).
[17]R. A. Street, Solid State Commun. **24**, 363 (1977).
[18]Weiqing Zhou, D. E. Sayers, M. A. Paesler, B. Bouchet-Fabre, Q. Ma, and D. Raoux, Phys. Rev. B **47**, 686 (1993).
[19]P. H. Fuoss, P. Eisenberger, W. K. Warburton, and A. Bienenstock, Phys. Rev. Lett. **46**, 1537 (1981).
[20]Sasaki (unpublished).
[21]R. W. James, *The Optical Principles of the Diffraction of X-rays* (Bell, London, 1954), p. 93.
[22]B. W. Warren, *X-ray Diffraction* (Addison-Wesley, Reading, MA, 1969), p. 127.
[23]Weiqing Zhou, Ph.D. thesis, North Carolina State University, 1991 (unpublished).
[24]Q. Ma, D. Raoux, and S. Benazeth, Phys. Rev. B **48**, 16 332 (1993).
[25]N. Morimoto, Mineral. J. (Sapporo) **1**, 160 (1960); J. E. D. Mullen and W. Nowaki, Z. Kristallogr. **136**, 48 (1972).
[26]N. F. Mott and A. M. Stoneham, J. Phys. C **10**, 3291 (1977).
[27]M. Kastner, D. Adler, and H. Fritzsche, Phys. Rev. Lett. **37**, 1504 (1976).
[28]V. L. Averianov, A. V. Kolobov, B. T. Kolomiets, and V. M. Lyubin, Phys. Status Solidi A **57**, 81 (1980); J. Non-Cryst. Solids **45**, 343 (1981).
[29]Ke Tanaka, in *Structure and Excitation of Amorphous Solids,* edited by G. Lucovsky and F. L. Galeener, AIP Conf. Proc. No. **31**, 1976, p. 148; in *Fundamental Physics of Amorphous Semiconductors,* edited by F. Yonezawa (AIP, New York Springer, Berlin, 1981), p. 104.
[30]S. Ernst, M. Rosendauer, U. Schwarz, P. Deak, K. Syassen, M. Stutzmann, and M. Cardona, Phys. Rev. B **49**, 5362 (1994).
[31]S. Ernst, M. Rosendauer, U. Schwarz, P. Deak, K. Syassen, M. Stutzmann, and M. Cardona, Phys. Rev. B **49**, 5362 (1994).
[32]B. Cabane and J. Friedel, J. Phys. (Paris) **32**, 73 (1971); M. Cutler, J. Non-Cryst. Solids **21**, 137 (1976).
[33]A. Mellene, R. Bellissent, and A. M. Flank, Europhys. Lett. **4**, 705 (1987).
[34]Ke Tanaka, J. Non-Cryst. Solids **59&60**, 925 (1983).
[35]J. P. Deneufville, S. C. Moss, and S. R. Ovshinsky, J. Non-Cryst. Solids **13**, 191 (1976).
[36]S. R. Elliott, Phys. Rev. Lett. **67**, 711 (1991); Nature **354**, 445 (1991).
[37]P. Armand, A. Ibanez, E. Philippot, Q. Ma, and D. Raoux, J. Non-Cryst. Solids **150**, 371 (1992).
[38]V. Halpern, Philos. Mag. **34**, 321 (1976).
[39]M. Frumer, A. P. Firth, and A. E. Owen, Philos. Mag. B **50**, 463 (1984).
[40]Ke Tanaka, Jpn. J. Appl. Phys. **25**, 779 (1986).